



Graphite and carbon black materials as catalysts for wet peroxide oxidation

C.M. Domínguez ^{a,*}, P. Ocón ^b, A. Quintanilla ^a, J.A. Casas ^a, J.J. Rodriguez ^a

^a Área de Ingeniería Química, Universidad Autónoma de Madrid, Campus de Cantoblanco, 28049 Madrid, Spain

^b Departamento de Química Física Aplicada, Facultad de Ciencias Químicas, Universidad Autónoma de Madrid, Campus de Cantoblanco, 28049 Madrid, Spain

ARTICLE INFO

Article history:

Received 12 June 2013

Received in revised form 26 July 2013

Accepted 30 July 2013

Available online 9 August 2013

Keywords:

Carbon black

Graphite

Hydrogen peroxide

Catalytic wet peroxide oxidation

Cyclic voltammetry

ABSTRACT

This study explores the application of non-porous carbon materials, two graphites (G-F, G-S) and two carbon blacks (CB-V and CB-C) as catalysts for wet peroxide oxidation (CWPO). The activity, efficiency and stability of these carbon materials have been evaluated using phenol as target compound. The catalyst screening experiments were carried out batch-wise at $C_{\text{Phenol},0} = 1 \text{ g/L}$, $C_{\text{H}_2\text{O}_2,0} = 5 \text{ g/L}$, $C_{\text{cat}} = 2.5 \text{ g/L}$, $T = 80^\circ\text{C}$ and $\text{pH}_0 = 3.5$. The results allow concluding that CB-C was the most stable catalyst, although it showed a lower oxidation and mineralization activity than G-S and CB-V. Increasing the temperature up to 90°C allowed complete phenol conversion and around 70% TOC reduction with 100% efficiency of hydrogen peroxide consumption upon 20 h reaction time at 5 g/L CB-C load. As a consequence of the initial oxidation of the carbon surface, the electrochemical properties of CB-C were favorably changed upon CWPO and its catalytic performance was improved from the first to the second use and then maintained upon successive applications in a five-cycle test.

© 2013 Elsevier B.V. All rights reserved.

1. Introduction

Catalytic wet peroxide oxidation (CWPO) relies on the oxidation of organic water pollutants with hydroxyl and hydroperoxyl radicals produced upon decomposition of hydrogen peroxide in the presence of a catalyst, typically iron, under working temperatures of 50–130 °C and pressures of 1–5 atm. Homogeneous CWPO technology has been commercialized under different proprietary processes, US Peroxide, OXY-PURE®, OHP® and PROX T.E.C [1]. These commercial systems are attractive because of their simple design and cost-effective operation. The disadvantages of homogeneous CWPO are the sensibility to pH, which must be always within the 2.5–3.5 range and the continuous loss of the dissolved iron catalyst which moreover needs to be separated from the effluent to avoid additional pollution. These issues have driven the investigation of active and stable solid catalysts, which has resulted in a growing literature on heterogeneous CWPO. A comprehensive survey of recent research on solid catalysts for CWPO is provided in the reviews of Perathoner and Centi [2], Garrido-Ramírez et al. [3], Navalón et al. [4] and Dhaskshinamoorthy et al. [5]. According to them, most CWPO studies are devoted to the incorporation of Fe, Mn, Co or Cu, as oxide species, metal complexes or

in the form of nanoparticles on different supports, such as zeolites, mesostructured materials, silica, alumina, pillared clays and activated carbons. Some studies with supported noble metals such as Pt, Ru, Pd and Au, have been also recently published [1,6,7]. It must be highlighted the difficulty of comparing the results on the activity of the different catalysts since specific operating conditions, i.e. pH, pollutant/catalyst ratio, temperature, amount of hydrogen peroxide and the way of feeding it to the wastewater have been used.

The difficulty of developing suitable catalysts is noticed in the literature. Finding efficient and stable catalysts allowing detoxification of wastewater upon reasonable reaction times is an important challenge. Solid catalysts are usually unstable in the long term because of the leaching of the active phase as a consequence of the low pH caused by the presence of organic acids as by-products which also can give rise to the formation of metal complexes, particularly with oxalic acid [8,9].

The catalytic efficiency is associated to the selectivity for hydrogen peroxide decomposition into active hydroxyl and hydroperoxyl radicals, capable of breaking-down the organic pollutants instead of being consumed in un-productive (parasite) reactions. Efficient catalysts are desirable to provide the maximum TOC removal per unit of hydrogen peroxide, a crucial issue for the economy of the system. This concept is receiving increasing attention in the literature [10–13]. The interest for stable catalysts avoiding metal leaching has promoted the exploration of bare carbon materials, whose lower activity, compared to metal-bearing catalysts, can be

* Corresponding author. Tel.: +34 914975602; fax: +34 914973516.

E-mail addresses: carmenmaria.dominguez@uam.es, cm.domingueztorre@gmail.com (C.M. Domínguez).



compensated by working at higher loads, which does not represent a drawback if they can be purchased at a lower cost. Activated carbons have been the most commonly used carbon materials in CWPO [4,8,14–22]. They exhibit donor-acceptor surface properties. The electron-rich sites such as basic surface oxygen groups and basal planes allow hydrogen peroxide decomposition into radical species through an electron transfer reaction similar to the Fenton mechanism [23]. Their efficiency for the decomposition of hydrogen peroxide is highly dependent on the adsorption of the organic pollutants, as recently demonstrated by Dominguez et al. [22]. In that work, unprecedented hydrogen peroxide efficiencies of almost 100% were reported for the CWPO of phenol with activated carbons. Under the selected reaction conditions (high pollutant concentration, 5 g/L of phenol and pollutant/carbon mass ratio = 2), great part of the carbon surface was occupied by phenol and the amount of available active sites was reduced. As a consequence, better controlled hydrogen peroxide decomposition into hydroxyl and hydroperoxy radicals was achieved and these species efficiently reacted with phenol in the vicinity of the carbon surface, reducing parasitic recombination and allowing a more efficient consumption of hydrogen peroxide. Catalyst stability was an important issue analyzed in that work. The activated carbon showed a progressive deactivation upon successive uses as a consequence of condensation by-products formed on the carbon surface. The activity was easily recovered by oxidative thermal regeneration (350 °C, 24 h).

In the current work, we explore the application of other carbon materials such as graphite and carbon black, of much lower surface area that can be available at reasonable low cost. The activity of these carbon materials for hydrogen peroxide decomposition was already demonstrated in a previous work [23]. The purpose of the present study is to evaluate their activity, efficiency and stability in CWPO using phenol as target compound. It is expected that with these materials of low adsorption capacity, deactivation by adsorbed condensation by-products can be avoided, or greatly reduced.

To the best of our knowledge, there are no previous studies on the application of carbon blacks for CWPO, whereas graphites have been scarcely studied in that process yielding in general fairly poor results [14,24].

2. Experimental

2.1. Reagents

Aqueous phenol solutions were prepared (1 g/L) (Sigma-Aldrich) at pH = 3.5 (HCl, Panreac). Hydrogen peroxide solution (30%, w/w) was purchased from Sigma-Aldrich. Working standard solutions of phenol, hydroquinone, resorcinol, catechol, *p*-benzoquinone, acetic acid, formic acid, malonic acid, maleic acid all from Sigma-Aldrich and oxalic acid (Panreac) were prepared and used for high performance liquid chromatography (HPLC) and ionic chromatography (IC) calibration. Other reagents used in the analyses were H₂SO₄ (Panreac), C₂H₃N (Riedel-deHaën), Na₂CO₃ (Panreac), NaHCO₃ (Merck), Na₂S₂O₈ (Panreac), HPO₄ (Fisher), C₆H₄COOHCOOK (Aldrich), TiOSO₄ (Riedel-deHaën). All these reagents were of analytical grade and were used without further purification. All the solutions were prepared with milli-Q water.

2.2. Catalysts

Commercial graphites, supplied by Fluka (G-F, ref.: 1249167) and Sigma-Aldrich (G-S, ref.: 282863) and two carbon blacks, supplied by Chemviron (CB-C, ref.: 2156090) and Vulcan (CB-V, ref.: CC72R) were tested as catalysts for CWPO of phenol. All samples were provided in powder form.

2.3. Catalyst characterization

Structural characterization of the carbon materials by powder X-ray diffraction (XRD) was carried out in a Siemens Model D5000 X-ray diffractometer, using Cu K α (8.04 keV) radiation and a step of 0.02°/s for 2θ = 5–100° and analyzed with PDF 2000 (JCPDS-ICDD) software.

The specific surface area (S_{BET}) values were obtained from the N₂ adsorption/desorption isotherms at 77 K using a Micromeritics Tristar apparatus on samples previously outgassed overnight at 150 °C to a reduced pressure <10⁻³ Torr in order to ensure a dry clean surface. The external or non-microporous surface area (A_{ext}) was calculated by the *t*-method. Elemental analyses were performed in a LECO Model CHNS-932 analyzer. Element identification in the carbon ashes was carried out by TXRF (Extra-II Rich & Seifert spectrometer). The amount of surface oxygen groups (SOG) in the carbons was accomplished by Temperature-programmed desorption (TPD) under N₂ (1000 NmL/min) as carrier gas. A carbon sample of 100 mg was placed in a quartz tube and heated at 10 °C/min from room temperature up to 900 °C. The evolved CO₂ and CO were measured by a SIEMENS gas analyzer (mod. Ultramat 22). Peaks deconvolution of the TPD spectra were adjusted to multiple Gaussian function by Peakfit 4.12 software.

Thermal gravimetric analyses (TGA) were performed on a Mettler-Toledo TGA/SDTA 851^e thermobalance in air atmosphere from 50 to 900 °C (10 °C/min).

Cyclic voltammetry (CV) measurements were carried out in a conventional three-electrode electrochemical cell, using a computerized potentiostat (Autolab PGSTAT 302, Eco Chemie). A glassy carbon electrode was used as substrate for the carbon samples, a gold electrode as the counter, a saturated Ag/AgCl, KCl electrode as the reference and HCl solution (pH = 3.5) as electrolyte. 20 μL of the carbon suspension (6 mg of carbon in 730 μL Milli-Q water) was dropped on the glassy carbon electrode to obtain a uniform film and subjected to CV (10 mV/s) under nitrogen atmosphere in the absence and presence of hydrogen peroxide (25 g/L) in the potential range from -0.6 to 1 V. From these measurements, the coulombic charge (CC) and the exchange current (i_0) were calculated. More detailed description of these tests has been reported elsewhere [23].

2.4. CWPO experiments

The CWPO runs were carried out batch-wise in a magnetically stirred three-necked glass reactor equipped with a reflux condenser. In a typical experiment, 45 mL of phenol solution (1 g/L) at pH = 3.5 (HCl) were placed in the reactor, along with the selected mass of carbon (0–0.375 g) and heated up to the desired temperature (80–90 °C). After that, 5 mL of an adjusted concentration of hydrogen peroxide aqueous solution were added and the stirring at 1200 rpm started. Effluents at different reaction times were taken from the reactor and immediately analyzed. After 24 h of reaction, the heating was switched-off and the reactor cooled to room temperature in cold water. Then, the catalyst was separated by filtration (0.45 μm Nylon filter) and dried at 60 °C. A blank experiment was carried out to assess the homogenous contribution. Phenol adsorption runs were performed at the same operating conditions as the oxidation tests but without hydrogen peroxide addition. The initial pH was set at 3.5 which is within the range most commonly reported in the literature for CWPO with iron catalysts [2]. All the experiments were performed by triplicate being the standard deviation always less than 5%.

Table 1

Structural and textural characterization and phenol adsorption of graphites and carbon blacks.

Sample	d_{002} (nm)	L_c (nm)	L_a (nm)	S_{BET} (m^2/g)	A_{ext} (m^2/g)	mg Ph/g C
G-F	0.337	46.63	48.87	6	6	6.44
G-S	0.338	44.09	48.70	12	12	13.88
CB-C (fresh)	0.348	7.08	6.57	75	67	27.20
Used CB-C	—	—	—	53 ^a	49 ^a	—
CB-V (fresh)	0.362	3.87	3.89	233	110	152.6
Used CB-V ^b	—	—	—	115	111	—

^a 1st use after 24 h reaction.^b 4th use after 24 h reaction.

2.5. Analytical methods

Phenol and aromatic intermediates were identified and quantified by means of HPLC (Varian, Mod. ProStar) by a Nucleosil C18 5 mm column (Microsob-MV, 15 cm length, 4.6 mm diameter) using a mixture of 4 mM H_2SO_4 aqueous solution at 1 mL/min as mobile phase. A diode array detector (PDA detector) at wavelengths of 210 and 246 nm was used. Short-chain organic acids were determined by IC (Metrohm, mod. 883 BASIC IC Plus) with anionic chemical suppression using a conductivity detector. A Metrosep A supp 5-250 column (25 cm length, 4 mm diameter) was used as stationary phase and 0.7 mL/min of an aqueous solution 3.2 mM of Na_2CO_3 and 1 mM of NaHCO_3 as mobile phase. Total organic carbon was measured with a TOC analyzer (Shimadzu TOC V_{SCN}). Hydrogen peroxide concentration and iron in solution were determined by colorimetric titration with a UV 2100 Shimadzu UV-VIS spectrophotometer using the titanium sulfate [25] and o-phenanthroline [26] methods, respectively.

3. Results and discussion

3.1. Catalyst characterization

The structural and textural characteristics of the graphites (G-S and G-F) and carbon blacks (CB-C and CB-V) are summarized in Table 1. The XRD profiles and N_2 adsorption-desorption isotherms of the four carbon materials tested along with the pore distribution of the carbon blacks are included as Supporting Information (Figures S1, S2 and S3, respectively). The C percentage from elemental analysis and the ash content along with the results from TPD are collected in Table 2.

As expected, the graphitic carbons show significantly higher structural order than the carbon blacks with much more developed crystalline domains as can be seen from the height (L_c) and width (L_a) dimensions calculated from the XRD profiles. The interlayer spacing value (d_{002}) of the two graphites is very close to the standard value (0.335 nm). Both graphites yielded very similar values of the crystalline structural parameters whereas some significant differences can be observed between the two carbon blacks.

Table 2

Elemental C (% d.a.f.), ash content (% d.b.) and surface oxygen groups of the carbon materials tested.

Sample	C (%)	Ashes (%)	CO_2 ($\mu\text{mol/g}$)	CO ($\mu\text{mol/g}$)
G-F	96.6	0.2	128	79
G-S	97.2	0.5	105	36
CB-C	≈99	0.0	83	214
1st use CB-C	98.4	0.0	197 ^a /201 ^b	226 ^a /256 ^b
CB-V	97.1	0.85	148	137
1st use CB-V	92.9	0.85	413	729

d.a.f., dry-ash-free basis; d.b., dry bases.

^a 1st use after 24 h reaction.^b 4th use after 24 h reaction.

The graphites showed fairly low values of BET surface area (Table 1). This was also the case of CB-C carbon black, although with significantly higher specific area and some developed porosity due to the presence of narrow mesopores. Meanwhile, the CB-V carbon black, with substantially higher BET surface area, presents an important contribution of microporosity as well as narrow mesopores.

As expected, the chemical composition of these materials consists essentially of C (Table 2). Some low amounts of O are accompanying as surface oxygen groups (SOGs) (Table 2). The graphites contain majorly acidic CO_2 -evolving SOGs whereas CB-C mostly presents CO-evolving SOGs. CB-V, with fairly similar amount of SOG as CB-C, contains both types of SOGs in about the same proportion (more detailed SOGs assessment is given in Table S1 of Supporting Information). The ash content was very low in all cases and almost negligible for CB-C (Table 2). Noteworthy, iron, the most critical ash constituent regarding CWPO, due to its widely demonstrated catalytic activity, was only present in G-S. According to TXRF analyses, this material contains 0.4 wt% of Fe. The non-negligible ash content in CB-V sample (0.85%, Table 2) is constituted mainly by Al, inert metal in CWPO processes.

The adsorption of phenol was checked (1 g/L phenol was stirred with 2.5 g/L carbon at 80 °C during 4 h), and the values are included in Table 1. As can be seen, the adsorption values vary consistently with the specific area being much higher for the CB-V carbon black. As indicated before, it would be desirable to use carbon materials with low phenol adsorption capacity with the aim of minimizing or even avoiding the formation of condensation products on the surface, which provokes deactivation [22]. Taking the reference of Panreac activated carbon (#:121237), which adsorbs 200 mg of phenol per gram of carbon under the same conditions, all the carbon materials tested in this study, except CB-V, yielded much lower adsorption.

3.2. Catalyst activity

The conversions of phenol, TOC and hydrogen peroxide achieved with each carbon upon CWPO after 4 h reaction time are given in Fig. 1. The removal of phenol achieved in the absence of hydrogen peroxide has been also included for the sake of discrimination between adsorption and reaction. Except in the case of CB-V, the contribution of adsorption is of very low significance, especially for graphites. As observed, all the carbon materials tested promoted the decomposition of hydrogen peroxide, showing different catalytic activity, which in terms of phenol conversion and partial mineralization follows the order: G-S > CB-V > CB-C > G-F.

The much higher catalytic activity of graphite G-S versus G-F in spite of their quite similar characteristics can be explained by the iron content of the former (0.4 wt%). In addition, 1.5 mg/L of Fe were detected in the liquid phase after 4 h reaction time with this graphite so that the homogeneous contribution of iron leached should not be discarded. To check this issue, a control experiment was carried out by removing the graphite after 1 h of reaction and continuing the reaction with the filtrate (where the leached Fe was

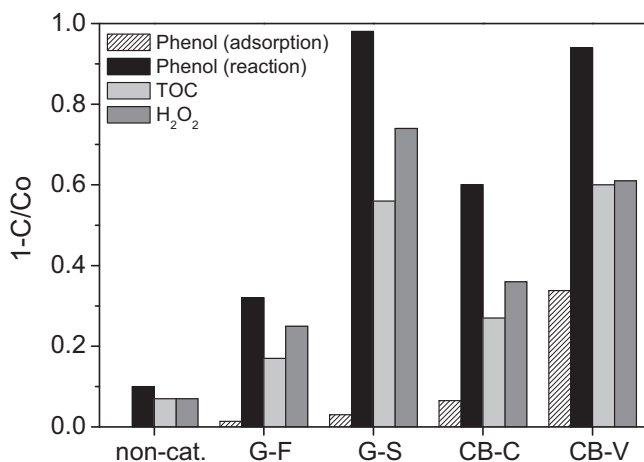


Fig. 1. Phenol disappearance (by adsorption and reaction), TOC removal and H₂O₂ decomposition after 4 h of reaction. Operating conditions: $C_{\text{Phenol},0} = 1 \text{ g/L}$, $C_{\text{H}_2\text{O}_2,0} = 5 \text{ g/L}$, $C_{\text{cat}} = 2.5 \text{ g/L}$, $T = 80^\circ\text{C}$ and $\text{pH}_0 = 3.5$.

dissolved), during another 3 h. Eventually, similar phenol and TOC conversions as those obtained in presence of the G-S (Fig. 1) were observed, allowing to conclude that the activity observed with this catalyst is predominately due to the Fe leached.

With regard to carbon blacks, none of them contain Fe neither other active metallic ashes, and therefore, the carbon structure (electron-rich sites such as basic surface oxygen groups and basal planes) is the only responsible of the activity. As can be seen, CB-V showed a higher activity (*ca.* 93% phenol, 60% TOC and 60% hydrogen peroxide conversions) than CB-C due to its higher specific surface area which implies a higher amount of active sites for hydrogen peroxide decomposition [23].

3.3. Catalyst efficiency

The time-evolution of TOC removal and hydrogen peroxide consumption with the tested materials are given in Fig. 2. The mineralization curves follow a trend consistent with that of the hydrogen peroxide, the TOC disappearance being faster during the first 4 h of reaction, when phenol and aromatic intermediates breakdown to low-weight carboxylic acids and CO₂. In the case of CB-V, the TOC removal values at reaction times below 4 h are higher than those of H₂O₂ decomposition, which can be explained only by considering the adsorption contribution.

The efficiency of hydrogen peroxide, calculated as $X_{\text{TOC}}/X_{\text{H}_2\text{O}_2}$ [11], upon reaction time is depicted in Fig. 3. As observed, that efficiency increased with reaction time up to asymptotic values (90% for graphites and 100% for carbon blacks). In the early stages, the decomposition of hydrogen peroxide catalyzed by the carbon surface leads to high concentrations of hydroxyl radicals that favor parasite scavenging reactions. As hydrogen peroxide is consumed and the aromatic intermediates oxidized (visualized by the color change of the samples from brownish to colorless), the surface concentration of radical species decreases and the parasitic recombination is progressively reduced thus increasing the efficiency of H₂O₂ toward oxidation and eventually mineralization. The hydrogen peroxide efficiency at short reaction times can be improved by optimizing the operating conditions, as will be later demonstrated for the CB-C catalyst.

3.4. Catalyst stability and reusability

The most active carbon materials, *viz.* G-S, CB-V and CB-C, were tested in successive CWPO runs in order to analyze their stability.

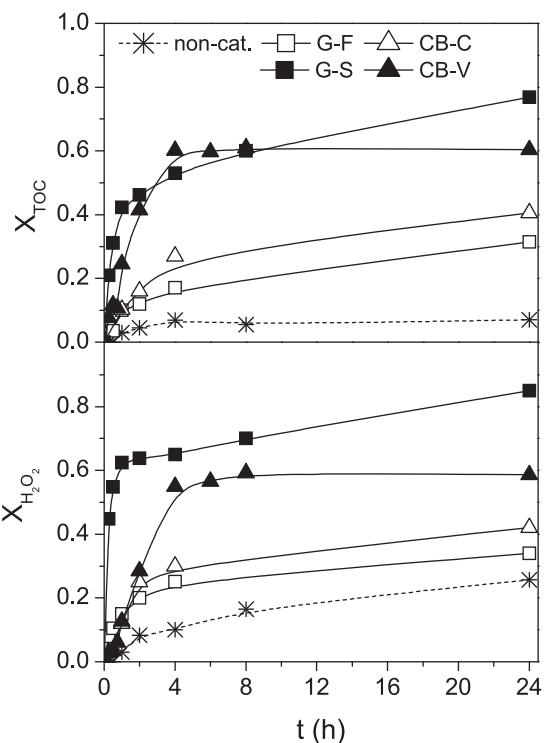


Fig. 2. TOC and H₂O₂ conversion profiles at the operating conditions of Fig. 1.

G-F was discarded for further studies because of its low activity in CWPO of phenol (Fig. 1). In each cycle, the catalyst was used during 24 h in reaction, then separated by filtration and dried at 60 °C for another 24 h before being used again in a new cycle. The phenol, TOC and hydrogen peroxide conversion values at 4 and 24 h reaction time upon successive cycles are given in Fig. 4a and b. The initial activity of G-S and CB-V decreased upon successive cycles, in particular for CB-V (Fig. 4a), though at higher phenol conversions that effect was significantly attenuated (Fig. 4b), those carbons recovered in part their performance and the differences with the more stable CB-C became much lower. In the case of G-S, the content of Fe was reduced by 15% from the first to the second use (due to leaching) and no further loss of Fe was detected in successive cycles. As indicated before, the activity of this carbon must be greatly

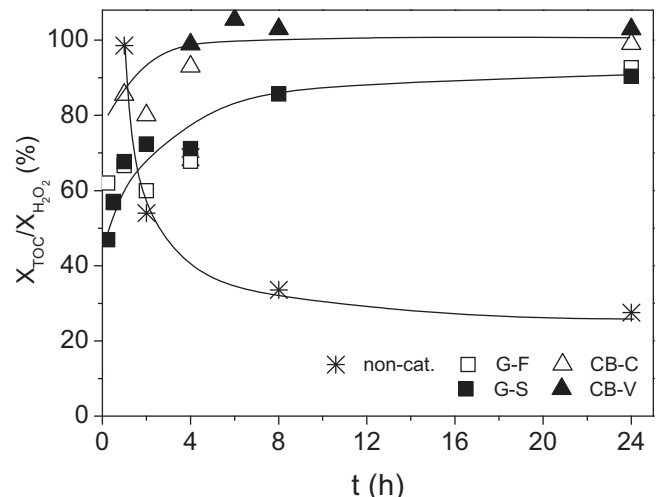


Fig. 3. Evolution of the efficiency of hydrogen peroxide consumption upon reaction time at the operating conditions of Fig. 1.

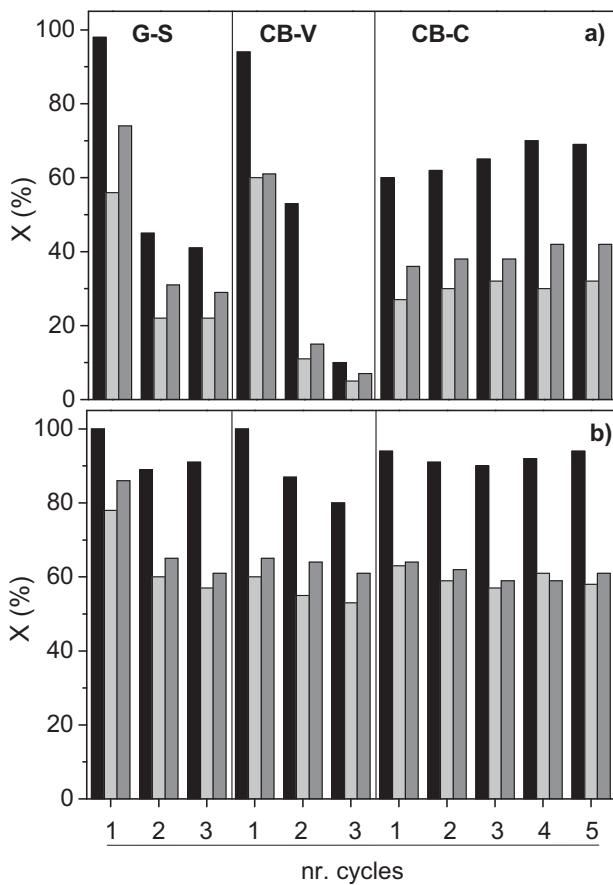


Fig. 4. Performance of the catalyst upon successive uses at 4 h (a) and 24 h (b) reaction time (X_{phenol} ■, X_{TOC} □ and $X_{\text{H}_2\text{O}_2}$ ■■). Operating conditions: $C_{\text{phenol},0} = 1 \text{ g/L}$, $C_{\text{H}_2\text{O}_2,0} = 5 \text{ g/L}$, $C_{\text{cat}} = 2.5 \text{ g/L}$ (G-S, CB-V) and 5 g/L (CB-C), $T = 80^\circ\text{C}$ and $\text{pH}_0 = 3.5$.

associated to the presence of iron as a main ash-component. Therefore, the decrease of iron content from the first to the second cycle and the absence of iron leaching (homogeneous contribution) in that second cycle can explain the decrease of the catalytic activity occurring only upon the two first uses.

The CB-V carbon black suffered almost complete deactivation after its second use (similar results were obtained in the third use

of this catalyst and in the blank experiment at a reaction time of 4 h, cf. Figs. 1 and 4a) but a significant recovery of activity was observed at higher reaction time (Fig. 4b) although with a monotonical decay upon successive cycles. Important changes were observed in this carbon black after its use in CWPO experiments (see Table 1). The BET surface area was reduced up to the value of the external area which remained unaltered, thus indicating almost complete blockage of the micropores, confirmed from pore size distribution (see Figure S3 of Supporting Information). Besides, the elemental analysis of the used carbon showed a significant reduction of C compared to the fresh one (see Table 2). These changes can be attributed to the presence of organic species, most probably oligomers from oxidative coupling reactions, on the carbon surface. The TPD results (Table 1) serve also to support this conclusion. As observed, the amounts of CO and CO_2 evolved upon TPD are substantially higher in the used catalyst than in the fresh one. The deconvolution of the TPD profiles and the assessment of the SOGs from those profiles are provided in the Supporting Information (Figure S4 and Table S1, respectively). As can be observed, CO_2 evolved mainly from carboxylic acid groups and CO from phenol and ether groups created upon CWPO.

TGA-DTG analyses of the fresh and used (3rd cycle) CB-V carbon black in air atmosphere are depicted in Fig. 5, where it can be observed a higher weight-loss percentage of the used CB-V (Fig. 5a) due to the burn-off of adsorbed species. The DTG profile after the 3rd cycle clearly shows a peak somewhat above 300°C (Fig. 5b). Formation of oligomeric condensation by-products on the carbon surface has been reported in a previous work on CWPO of phenol with activated carbons under similar operating conditions [22].

The CB-C carbon black showed no deactivation upon five successive cycles, where phenol conversion and TOC removal remained almost invariable. The efficiency of hydrogen peroxide consumption ($X_{\text{TOC}}/X_{\text{H}_2\text{O}_2}$) was maintained around 90% at the reaction times of Fig. 4. This suggests the absence of carbonaceous material adsorbed on the carbon surface, consistently with its low adsorption capacity. The TGA analyses confirmed this fact since similar weight-loss profiles were obtained for the fresh and 4th cycle CB-C (Fig. 5a) and the corresponding DTG curves did not show any peak (Fig. 5b).

Intriguingly, the initial performance of CB-C (Fig. 4a) showed a slight but monotonical improvement upon at least the first three cycles. The initial rate values depicted in Fig. 6 show a significant increase from the first to the second use of this carbon which then remained almost constant upon successive cycles. This initial

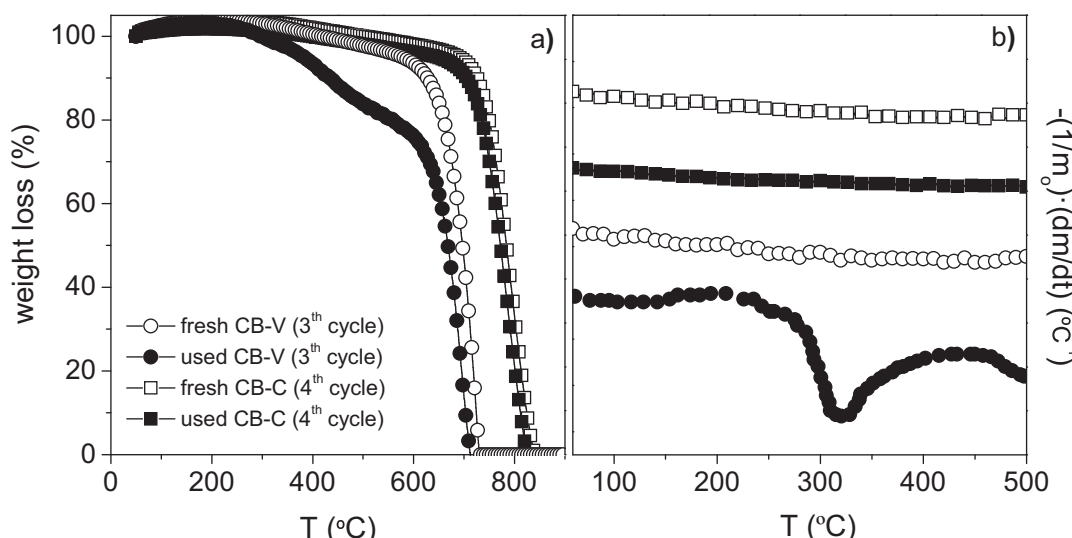


Fig. 5. TGA (a) and DTG (b) curves of fresh and used CB-V (3rd cycle), and fresh and used CB-C (4th cycle) in air at $10^\circ\text{C}/\text{min}$ heating rate.

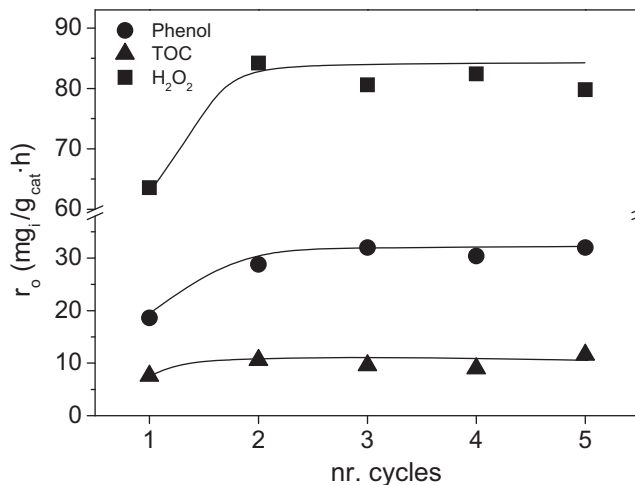


Fig. 6. Initial rates of phenol disappearance and TOC removal and hydrogen peroxide decomposition in sequential experiments over CB-C. Operating conditions: $C_{\text{Phenol},0} = 1 \text{ g/L}$, $C_{\text{H}_2\text{O}_2,0} = 5 \text{ g/L}$, $C_{\text{cat}} = 5 \text{ g/L}$, $T = 80^\circ\text{C}$ and $\text{pH}_0 = 3.5$. Initial rates calculated as $(r_o)_0 = (-dC_i/dt)_0/C_{\text{cat}}$.

increase is remarkably pronounced regarding to hydrogen peroxide decomposition.

To learn more on these results, cyclic voltammetry measurements of the fresh and used (2nd cycle) CB-C carbon black were carried out. The voltammograms obtained are presented in Fig. 7. The values of the coulombic charge (CC), calculated from Fig. 7a, and those of the exchange current (i_0), calculated from Fig. 7b, were 0.887 mC and 0.060 A/g, respectively, for the fresh carbon and 1.030 mC and 0.127 A/g for the used one. The evolution of the CC values indicates that the electrochemical capacity of CB-C increases upon its use in CWPO. The ability of CB-C to decompose hydrogen peroxide is enhanced after its use according to the increase of the i_0 value. In addition, the background voltammogram of the used CB-C shows two signals that were not present in the fresh carbon (Fig. 7a). The first signal occurs when the applied potential goes to positive direction, in the range from 0.1 to 0.3 V, while the second one appears when the potential goes to negative direction, from 0.3 to 0 V. Both signals, only present in the used carbon, can be attributed to the oxidation and reduction of SOGs, respectively. The creation of some SOGs upon CWPO is confirmed by the TPD analyses and seems to occur only in the early stages, likely due to the initial exposition to hydrogen peroxide. The amounts

of CO₂ evolved after the first use is significantly higher than from the fresh carbon and then remained almost constant (see Table 1). The SOGs formed are carboxylic acid and, in less extent, anhydride, ether and phenol (see Figure S3 and Table S1 of Supporting Information). The creation particularly of carboxylic acid groups confers some hydrophilic character to CB-C which was visualized by a better wettability of the solid when put in contact with aqueous phenol solution. This can favor the diffusion of the reagents to the active sites [27,28] and contribute to increase the carbon exchange current, enhancing the initial catalytic activity.

3.5. CWPO of phenol with CB-C

The preceding results support the potential application of the CB-C carbon black as a promising catalyst in CWPO. To learn more on its practical application, batch-wise experiments at different carbon loads, temperature and initial pH were performed.

Fig. 8 shows the time-evolution of phenol conversion and TOC removal at different catalyst loads (from 0 to 7.5 g/L), two temperatures (80 and 90 °C) and two initial pHs (3.5 and 6), always working at 1 g/L starting phenol concentration and the stoichiometric amount of hydrogen peroxide for complete mineralization. The positive effect of temperature can be clearly seen. Complete conversion of phenol was achieved at 90 °C but it required high catalyst load (5 g/L) and reaction times (around 20 h). Under these conditions, more than 70% mineralization was achieved. The remaining by-products were carboxylic acids, as can be seen in Fig. 9a. The highly toxic aromatic intermediates were completely converted upon 16 h reaction time. The values of TOC calculated from the species identified were always fairly close to the experimental TOC measurements (see Figure S5 of Supporting Information).

The efficiency of hydrogen peroxide consumption under the selected operating conditions of Fig. 8, is given in Fig. 10 where TOC removal versus H₂O₂ decomposition is depicted. The CB-C carbon allows a highly efficient consumption of hydrogen peroxide which is favored by increasing the temperature and the catalyst load. Therefore, these two issues enhance the selectivity toward oxidation inhibiting parasite scavenging reactions.

To check the influence of the initial pH, an experiment was performed at pH₀ = 6, T = 80 °C and C_{cat} = 5 g/L. The evolution of phenol and TOC conversions with reaction time is depicted in Fig. 8, while the hydrogen peroxide efficiency values achieved at these conditions are included in Fig. 10. As can be seen, phenol and TOC conversions were somewhat lower at pH = 6 at the beginning of the reaction, but similar results as those obtained at pH = 3.5

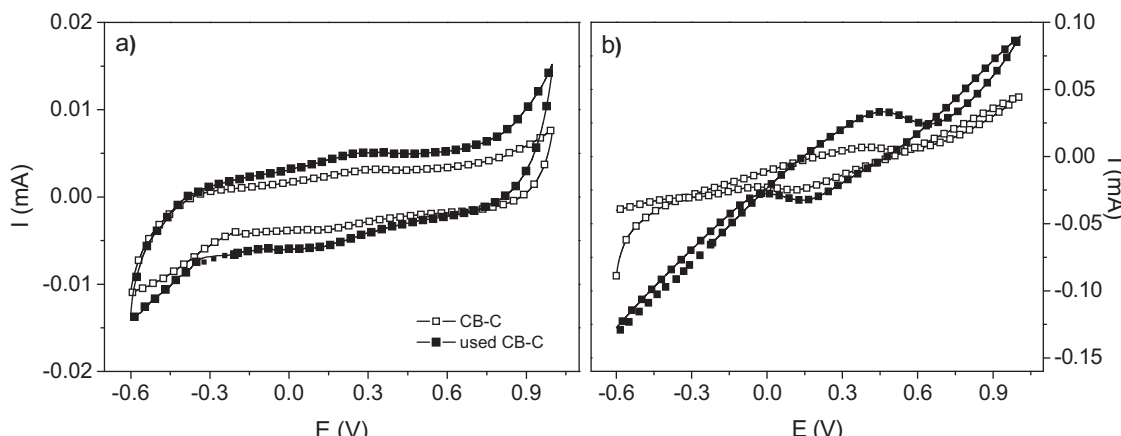


Fig. 7. Cyclic voltammograms of fresh and used CB-C in the absence (a) and the presence (b) of hydrogen peroxide. Operating conditions: $v = 10 \text{ mV/s}$, $T = 25^\circ\text{C}$, $\text{pH} = 3.5$ (HCl), $C_{\text{H}_2\text{O}_2} = 25 \text{ g/L}$.

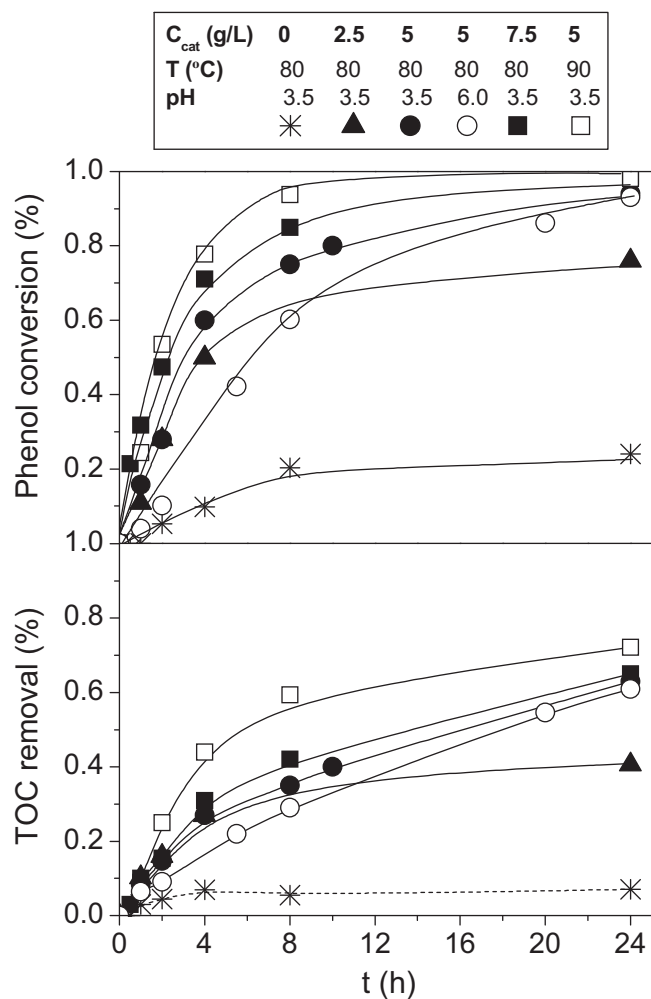


Fig. 8. Evolution of phenol and TOC upon reaction time in CWPO with the CB-C catalyst. Operating conditions: $C_{\text{Phenol},0} = 1 \text{ g/L}$, $C_{\text{H}_2\text{O}_2,0} = 5 \text{ g/L}$.

were achieved after 24 h. The hydrogen peroxide efficiency was maintained around 100%. Therefore, in this case, the pH is not a so critical variable as commonly reported for iron-catalyzed wet peroxide oxidation. This represents an important advantage when near-neutral effluents are treated since avoids pH adjusting.

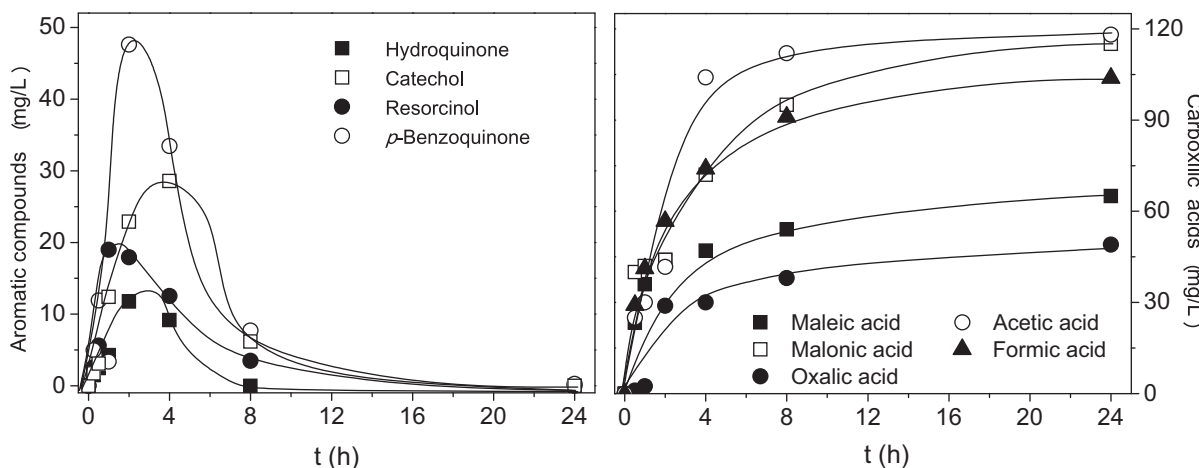


Fig. 9. Evolution of intermediates (a) and by-products (b) in CWPO of phenol with CB-C. Operating conditions: $C_{\text{Phenol},0} = 1 \text{ g/L}$, $C_{\text{H}_2\text{O}_2,0} = 5 \text{ g/L}$, $C_{\text{cat}} = 2.5 \text{ g/L}$, $T = 90^\circ\text{C}$ and $\text{pH}_0 = 3.5$.

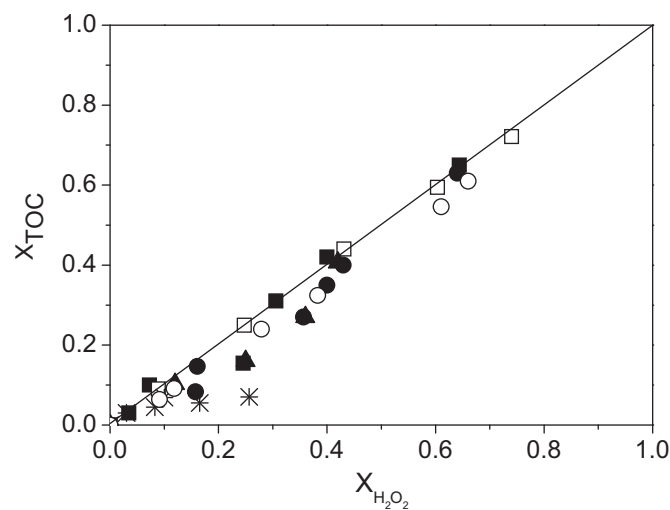


Fig. 10. TOC versus H_2O_2 conversions in CWPO of phenol with the CB-C catalyst at the operating conditions of Fig. 8 (symbols in Fig. 8).

4. Conclusions

Non-porous carbon materials with moderate specific area and without mineral impurities are efficient and stable catalysts for CWPO, as has been demonstrated by CB-C carbon black. This material presents sufficient electrochemical capacity to enable surface decomposition of hydrogen peroxide along with a low adsorption capacity to avoid or minimize the formation of adsorbed oligomeric by-products. Upon the early stages of the reaction, CB-C carbon black was oxidized resulting in an increased hydrophilic character which favored the diffusion of the reagents to the active sites, fact that contributed to increase the carbon exchange current, and therefore, its initial catalytic activity from its first to second use.

Complete conversion of phenol and around 70% TOC removal with 100% efficiency of hydrogen peroxide consumption were achieved in 20 h reaction time at moderate temperature (90°C) with high catalyst load (5 g/L) at 1 g/L starting phenol concentration and the hydrogen peroxide dose corresponding to the stoichiometric amount for phenol complete mineralization within the range of initial pH tested (3.5–6). The final by-products are low-weight carboxylic acids, of much lower ecotoxicity than the starting phenol and the aromatic oxidation intermediates.

Acknowledgments

The authors wish to thank the Spanish MICINN for the financial support through the projects CTQ2008-03988/PPQ and CTQ2010-14807. The Comunidad Autónoma de Madrid is also gratefully acknowledged for the financial support through the project S2009/AMB-1588.

Appendix A. Supplementary data

Supplementary data associated with this article can be found, in the online version, at <http://dx.doi.org/10.1016/j.apcatb.2013.07.069>.

References

- [1] A. Quintanilla, S. García-Rodríguez, C.M. Domínguez, S. Blasco, J.A. Casas, J.J. Rodríguez, *Applied Catalysis B: Environmental* 111 (2012) 81–89.
- [2] S. Perathoner, G. Centi, *Topics in Catalysis* 33 (2005) 207–224.
- [3] E.G. Garrido-Ramírez, B.K.G. Theng, M.L. Mora, *Applied Clay Science* 47 (2010) 182–192.
- [4] S. Navalón, A. Dhakshinamoorthy, M. Alvaro, H. Garcia, *Chemsuschem* 4 (2011) 1712–1730.
- [5] A. Dhakshinamoorthy, S. Navalón, M. Alvaro, H. Garcia, *Chemsuschem* 5 (2012) 46–64.
- [6] N.R. Sanabria, M.A. Centeno, R. Molina, S. Moreno, *Applied Catalysis A: General* 356 (2009) 243–249.
- [7] M.S. Yalfani, S. Contreras, F. Medina, J. Sueiras, *Applied Catalysis B: Environmental* 89 (2009) 519–526.
- [8] J.A. Zazo, J.A. Casas, A.F. Mohedano, J.J. Rodriguez, *Applied Catalysis B: Environmental* 65 (2006) 261–268.
- [9] J. Barrault, M. Abdellaoui, C. Bouchoule, A. Majesté, J.M. Tatibouët, A. Louloudi, N. Papayannakos, N.H. Gangas, *Applied Catalysis B: Environmental* 27 (2000) L225–L230.
- [10] J.A. Botas, J.A. Melero, F. Martínez, M.I. Pariente, *Catalysis Today* 149 (2010) 334–340.
- [11] J.A. Zazo, G. Pliego, S. Blasco, J.A. Casas, J.J. Rodriguez, *Industrial & Engineering Chemistry Research* 50 (2011) 866–870.
- [12] R. Martin, S. Navalón, M. Alvaro, H. Garcia, *Applied Catalysis B: Environmental* 103 (2011) 246–252.
- [13] N. Inchaurrondo, J. Cechini, J. Font, P. Haure, *Applied Catalysis B: Environmental* 111 (2012) 641–648.
- [14] F. Lücking, H. Köser, M. Jank, A. Ritter, *Water Research* 32 (1998) 2607–2614.
- [15] H.H. Huang, M.C. Lu, J.N. Chen, C.T. Lee, *Chemosphere* 51 (2003) 935–943.
- [16] A. Georgi, F.D. Kopinke, *Applied Catalysis B: Environmental* 58 (2005) 9–18.
- [17] A. Rey, M. Faraldo, A. Bahamonde, J.A. Casas, J.A. Zazo, J.J. Rodriguez, *Industrial & Engineering Chemistry Research* 47 (2008) 8166–8174.
- [18] V.P. Santos, M.F.R. Pereira, P.C.C. Faria, J.J.M. Orfao, *Journal of Hazardous Materials* 162 (2009) 736–742.
- [19] H.T. Gomes, S.M. Miranda, M.J. Sampaio, A.M.T. Silva, J.L. Faria, *Catalysis Today* 151 (2010) 153–158.
- [20] A. Dhaouadi, N. Adhoum, *Applied Catalysis B: Environmental* 97 (2010) 227–235.
- [21] F. Duarte, F.J. Maldonado-Hodar, L.M. Madeira, *Applied Catalysis B: Environmental* 103 (2011) 109–115.
- [22] C.M. Domínguez, P. Ocón, A. Quintanilla, J.A. Casas, J.J. Rodríguez, *Applied Catalysis B: Environmental* 140/141 (2013) 663–670.
- [23] C.M. Domínguez, A. Quintanilla, P. Ocón, J.A. Casas, J.J. Rodríguez, *Carbon* 60 (2013) 76–83.
- [24] S. Zrnčević, Z. Gomzi, *Industrial & Engineering Chemistry Research* 44 (2005) 6110–6114.
- [25] M. Eisenberg, *Industrial and Engineering Chemical Analysis* 15 (1943) 327–328.
- [26] E.B. Sandell, *Journal of Electroanalytical Chemistry* 1 (1959) 342.
- [27] O. Taran, E. Polyanskaya, O. Ogorodnikova, V. Kuznetsov, V. Parmon, M. Besson, C. Descorme, *Applied Catalysis A: General* 387 (2010) 55–66.
- [28] P. Hernández-Fernández, S. Baranton, S. Rojas, P. Ocon, J. Leger, J.L.G. Fierro, *Langmuir* 27 (2011) 9621–9629.